THE ASTROPHYSICAL JOURNAL, 395:L37–L40, 1992 August 10

ULTRAVIOLET IMAGING TELESCOPE ULTRAVIOLET IMAGES: LARGE-SCALE STRUCTURE, H II REGIONS, AND EXTINCTION IN M81

JESSE K. HILL,[1] RALPH C. BOHLIN,[2] KWANG-PING CHENG,[6,7] PAUL M. N. HINTZEN,[3,7,8]
WAYNE B. LANDSMAN,[1] SUSAN G. NEFF,[3] ROBERT W. O'CONNELL,[4] MORTON S. ROBERTS,[5]
ANDREW M. SMITH,[3] ERIC P. SMITH,[3,7] AND THEODORE P. STECHER[3]

Received 1992 March 31; accepted 1992 May 18

ABSTRACT

Ultraviolet images of M81 obtained by the Ultraviolet Imaging Telescope during the 1990 December *Astro-1* spacelab mission allow determination of 2490 and 1520 Å fluxes for 46 H II regions and global surface brightness profiles. Comparison photometry in the V band is obtained from a ground-based CCD image. Ultraviolet radial profiles show bulge and exponential disk components, with a local decrease in disk surface brightness inside the inner Lindblad Resonance $\sim 4'$ from the nucleus. The V profile shows typical bulge plus exponential disk structure, with no local maximum in the disk. There is little change of UV color across the disk, although there is a strong gradient in the bulge. The ratio of the near-UV surface brightness to the V band surface brightness in the disk is a factor ~ 4 lower for M81 than for M51. Total near-UV and far-UV UIT fluxes for M81 are consistent with previous measurements by *OAO 2*. The flux from the bulge is estimated to be 53% of the total in the V band, 31% in the near-UV, and 5% in the far-UV.

Observed m_{152}–V colors of the H II regions are consistent with model spectra for young clusters, after dereddening using A_v determined from $m_{249} - V$ and the Galactic extinction curve. The value of A_v, so determined, is 0.4 mag greater on the average than A_v derived from radio continuum and Hα fluxes. This difference is within the error estimates of the ground-based extinction determinations. The observed colors are unlikely to be caused by larger ages than the 3 Myr assumed by the model, since the Lyman continuum flux of a cluster is a strongly decreasing function of age.

Subject headings: ultraviolet: galaxies — galaxies: individual: M81 — ISM: H II regions

1. INTRODUCTION

Ultraviolet imagery of spiral galaxies is a sensitive probe of regions of active or recent star formation, where the emission is dominated by luminous hot massive stars. M81 is a well-known large, nearby grand-design Sb spiral galaxy and was a prime target for observation by the Ultraviolet Imaging Telescope (UIT) during the *Astro-1* spacelab mission in 1990 December. M81 (NGC 3031) was imaged in both near-UV and far-UV bandpasses during the mission. A ground-based CCD V band image was also obtained at Kitt Peak National Observatory (KPNO).

In § 2 we present and describe the ultraviolet and visual images obtained. In § 3 we discuss the overall morphology of M81 in the ultraviolet and the UV colors and reddening for H II regions, including comparison with the predictions of models. The results are summarized in § 4.

2. UIT AND GROUND-BASED IMAGES

The UIT instrument is described in detail by Stecher et al. (1992), who include plots of the wavelength dependence of the sensitivity of the near-UV and far-UV bandpasses used in observing M81. The UV bandpasses are centered at 2490 and 1520 Å, respectively, with widths 1150 and 354 Å. Three exposures were obtained in each bandpass, with exposure times about 25, 128, and 640 s for each camera. The resolution of the images is $\sim 3''$. Figures 1 and 2 (Plates L20 and L21) show $15' \times 15'$ subimages extracted from the longest near-UV and far-UV exposures, respectively. The 46 H II regions measured are circled on the near-UV (A1) image.

A description of the data reduction process, including digitization and subsequent processing which applies to all UIT images is given by Stecher et al. (1992). The calibration was determined using well-exposed *IUE* spectra of objects imaged by UIT during the Astro 1 mission, and is estimated to be accurate to about 10%. The magnitude m_{249} is related to the flux f_{249} by the relation $m_{249} = -2.5 \times \log (f_{249})$–21.10. A similar relation holds for m_{152} and f_{152}.

In addition, wide-field CCD images of M81 were obtained using the KPNO 0.9 m with the STIS2k (2048 × 2048 pixel) CCD and standard *BVRI* filter set. Figure 3 (Plate L22) shows a $15' \times 15'$ subimage extracted from the KPNO V image. A comparison of Figures 1–3 shows that the emitted flux is increasingly dominated by the star forming regions in the spiral arms as the wavelength decreases from 5500 Å(V) to 2490 Å(A1) to 1520 Å(B1).

3. ANALYSIS

3.1. *Large-Scale Structure*

Following Visser (1980a, b) and Leisawitz & Bash (1982), we adopt an inclination angle of 59° for M81 with a major axis position angle of 149°. Far-UV, near-UV, and V-band surface brightness profiles were obtained using as apertures a series of

[1] Hughes STX, 4400 Forbes Boulevard, Lantham, MD 20706.
[2] Space Telescope Science Institute, Homewood Campus, Baltimore, MD 21218.
[3] Laboratory for Astronomy and Solar Physics, NASA/GSFC, Greenbelt, MD 20771.
[4] University of Virginia, P.O. Box 3818, Charlottesville, VA 22903.
[5] National Radio Astronomy Observatory, Edgemont Road, Charlottesville, VA 22903.
[6] NASA/GSFC, NRC Postdoctoral Fellow, NASA/GSFC, Greenbelt, MD 20771.
[7] Visiting Astronomer at the Kitt Peak National Observatory of the NOAO operated by AURA, Inc., under contract to the NSF.
[8] Department of Physics and Astronomy, University of Nevada, Las Vegas, NV 89154.

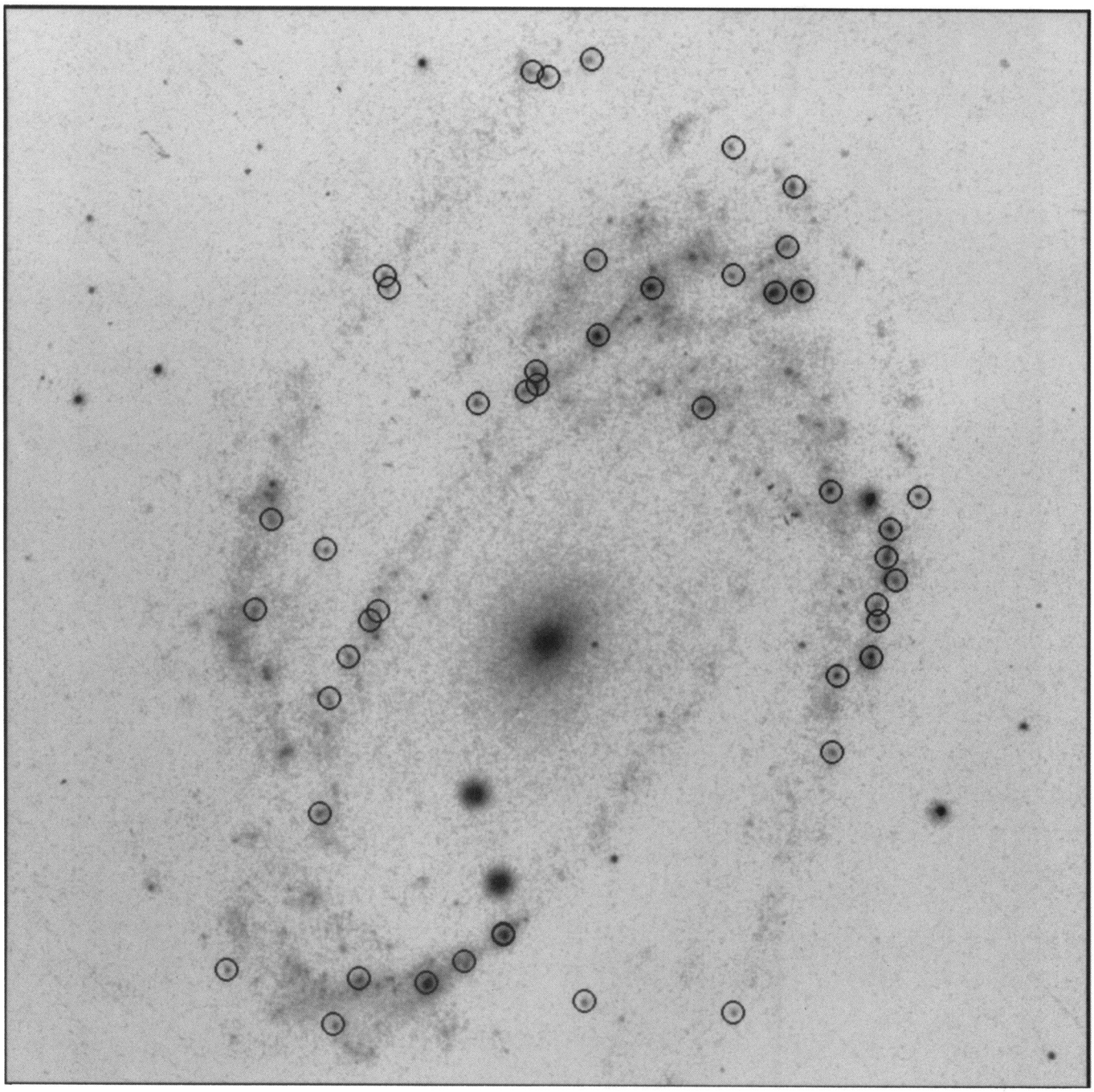

FIG. 1.—15′ × 15′ north-up, east-left section of A1 (near-UV, 2490 Å) image. The 46 H II region sources are circled.

HILL et al. (see 395, L37)

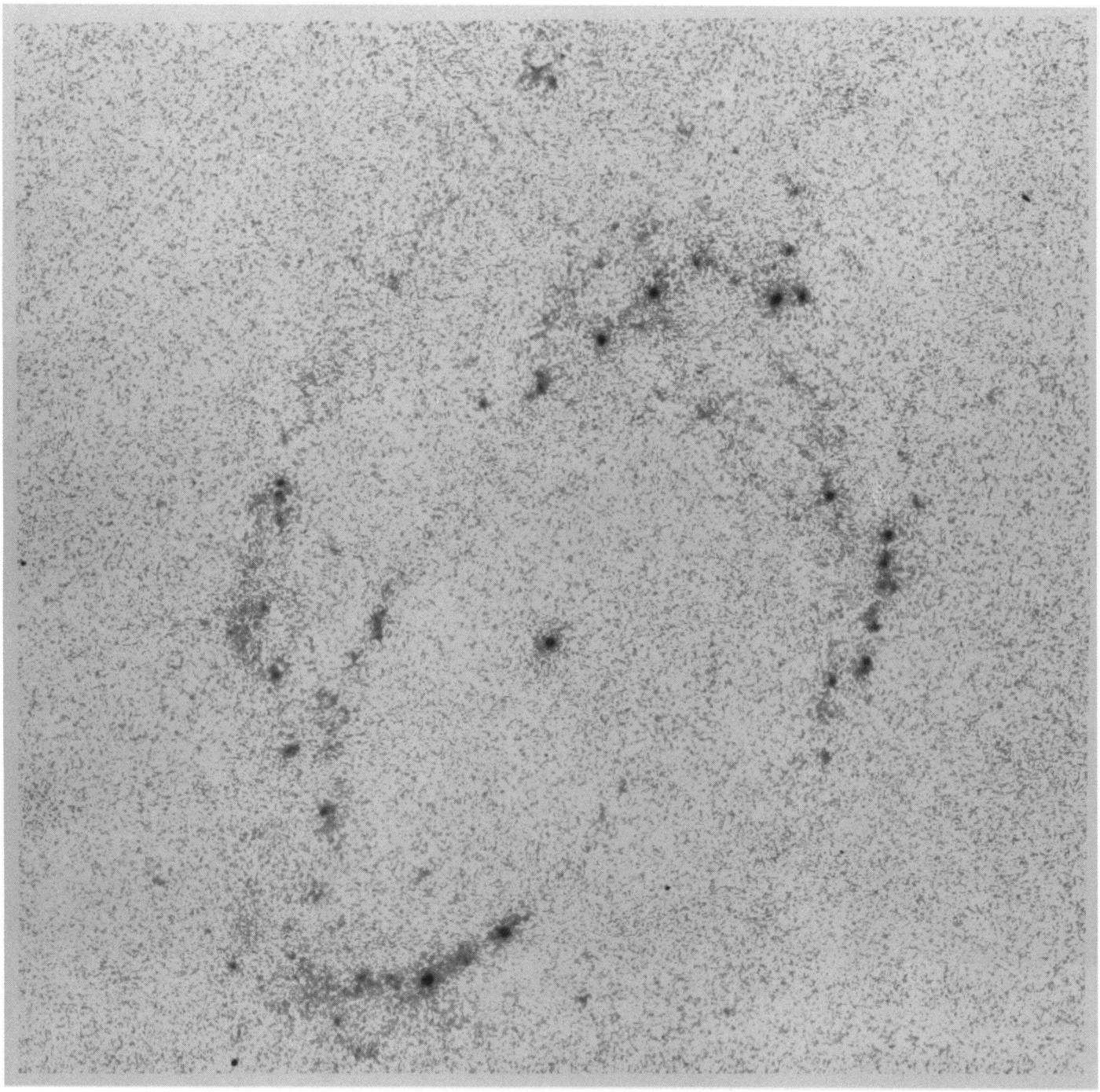

FIG. 2.—15′ × 15′ section of B1 (far-UV, 1520 Å) image, registered with Fig. 1

HILL et al. (see 395, L37)

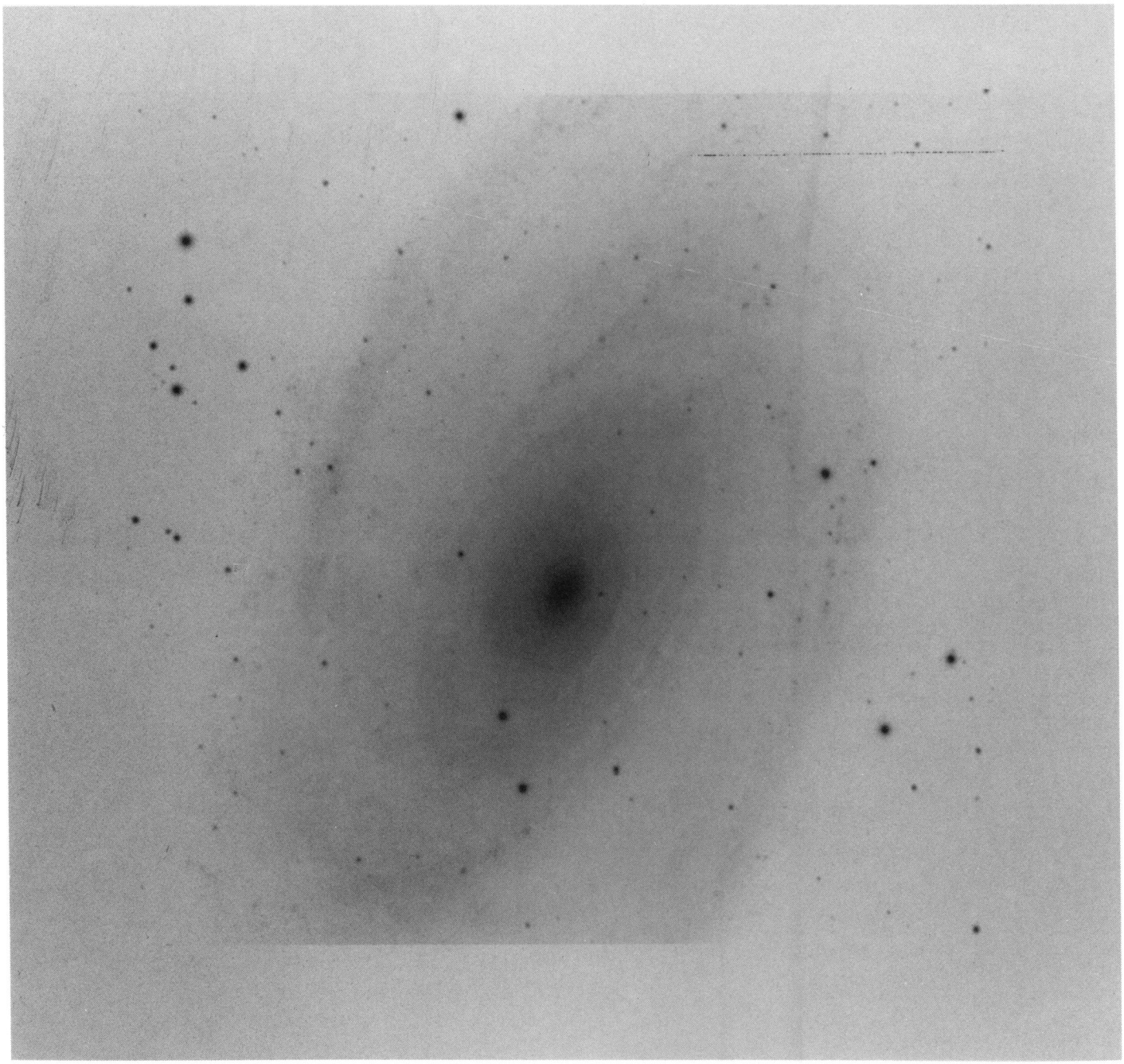

FIG. 3.—15′ × 15′ section of KPNO *V* image, registered with Fig. 1

HILL et al. (see 395, L37)

similar, nested elliptical annuli whose position angles and major-to-minor axis ratios were computed from the adopted inclination angle and major axis position angle. The semimajor axis of the annuli varied from 10″ to 740″ for the UIT images and from 10″ to 575″ for the smaller V image. No inclination-dependent corrections to the surface brightness were made. Global sky brightnesses in the UV bands are the averages over four 45″ square patches at the corners of a larger 11.3 square centered on the nucleus.

The radial profiles in the three bands are plotted in Figure 4. The V-band profile shows the bulge plus exponential disk morphology typical of spiral galaxies in ground-based optical bands (Freeman 1970; Boroson 1981), with a continuous decline outward and a relatively smooth transition between the two components. The UV radial profiles are different, in that the exponential disk appears to be attenuated interior to the inner Lindblad resonance (ILR), which occurs at a radius of about 4′ (Kaufman et al. 1989). The far-UV profile falls to below the sky level over the radius interval ~50″–200″, while the near-UV profile falls to a local minimum brighter than sky at about 3′ from the nucleus. Both UV profiles then increase to a maximum at a radius of about 5′ and fall exponentially at larger radii.

The result is a stronger distinction between the bulge and disk in the UV than in the optical and a dark annulus surrounding the bulge in the far-UV. This may result from inhibition of recent star formation inside the ILR. The inner galaxy is dominated by the bulge population, which exhibits a UV color gradient with the ratio of far-UV to near-UV surface brightness increasing towards the center. This gradient is discussed further in O'Connell et al. (1992), who provisionally attribute it to a gradient in metal abundance.

The size of any UV color gradient in the outer disk will depend sensitively on the adopted sky background of the far-UV image. Since the far-UV sky is very near the background fog level, the slope of the far-UV radial profile is not well-determined for distances from the nucleus greater than around 600″, corresponding to ~10 kpc for an assumed distance of 3.3 Mpc for M81. Nevertheless, it appears that any disk color gradients must be small. It is surprising that the disk, whose UV light is presumably sensitive to variations of the star-formation rate on time scales ~100 Myr, should have a more uniform UV color than the bulge, where old populations appear to dominate (O'Connell et al. 1992).

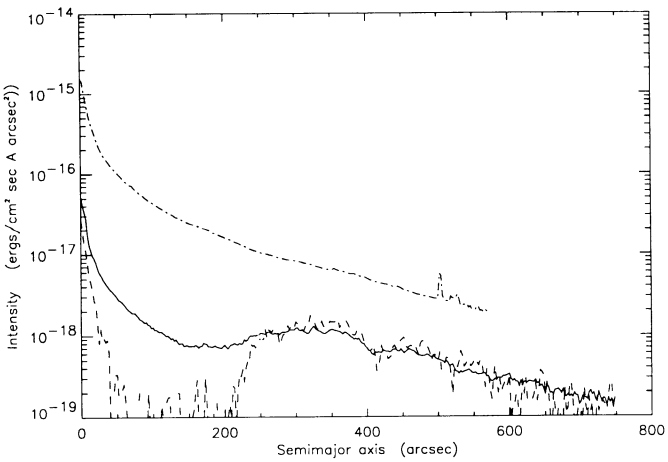

FIG. 4.—Radial surface brightness profiles in V (*dot-dashed line*), near-UV, (A1, *solid line*), and far-UV, (B1, *dashed line*).

Figure 4 shows that the UV disk color profile is essentially constant at $\mu_{152} - \mu_{249} \sim 0.0$ for radii greater than 5′. This corresponds approximately to the color of an A0 main-sequence star. The mean $m_{152} - m_{249}$ color for the 46 H II regions discussed later is −1.0, with rms deviation 0.4 mag, which is considerably bluer than the disk average. Disk UV light is evidently dominated not by the youngest stars, but rather by an intermediate age population formed over the past several Gyr. The 46 H II regions discussed later contribute 17% of the total disk flux in the far-UV and 8.6% of the total disk flux in the near-UV.

Our M81 surface brightness profiles may be compared with the radial surface brightness profiles for M51 in the near-UV, R, and U bands given by Bohlin et al. (1990). According to their Figure 2, compared with Figure 4 here, the maximum in the radial surface brightness profile for the arms plus disk in the near-UV band is $\sim 6.0 \times 10^{-18}$ ergs cm^{-2} Å^{-1} s^{-1} arcsec^{-2} in M51, but is only $\sim 1.0 \times 10^{-18}$ ergs cm^{-2} Å^{-1} s^{-1} arcsec^{-2} in M81. For M81 in the V band this quantity is $\sim 7.0 \times 10^{-18}$ ergs cm^{-2} Å^{-1} s^{-1} arcsec^{-2}. For M51 we estimate the V band flux as the average of the arms plus disk surface brightness maxima from the R and U band profiles, $\sim 1.0 \times 10^{-17}$ ergs cm^{-2} Å^{-1} s^{-1} arcsec^{-2}. Thus, the near-UV disk surface brightness is about factor of 6 lower for M81 than for M51, and the $m_{249} - V$ color of the disk of M81 is about 1.5 mag redder than that of M51. These differences are consistent with the higher star-formation rate now occurring in M51's disk.

The total UV fluxes of M81 in the far-UV and near-UV bands for $r < 10'$ are 3.9×10^{-13} ergs cm^{-2} Å^{-1} s^{-1} and 4.2×10^{-13} ergs cm^{-2} Å^{-1} s^{-1}, respectively, corresponding to magnitudes $m_{152} = 9.93$ and $m_{249} = 9.84$. We estimate the linearization and calibration errors to be less than 15%. However, increasing (decreasing) the far-UV sky background by 1 σ decreases (increases) the integrated far-UV flux by 50%. The total V band flux from the same region is 4.0×10^{-12} ergs cm^{-2} Å^{-1} s^{-1}.

The total bulge flux can be estimated roughly as the total flux from the regions with radius less than 200″. The bulge flux is thereby estimated at 53% of the total in the V band, 31% in the near-UV band, and 5% in the far-UV band, confirming the visual impression from Figures 1–3.

The *OAO 2* 1550 and 2460 Å band magnitudes, obtained using a 10′ diameter circular aperture, are ~9.7 and 10.3 ± 0.5, after correcting to the *IUE* flux scale (Code & Welch 1982), consistent with the UIT measurements.

3.2. H II *Regions*

Kaufman et al. (1987) observed M81 with the VLA at continuum wavelengths 6 and 20 cm. They used the radio continuum images together with Hα recombination line images obtained by Kennicutt & Hodge (1980) to identify 42 giant radio H II regions, measure the radio and Hα fluxes, and estimate the visual extinctions. They concluded that the average visual extinction of the giant H II regions is about 1.1 mag, with an estimated uncertainty of ±0.4 mag, and that there is little or no systematic gradient in the extinction as a function of distance from the nucleus.

Petit, Sivan, & Karachentsev (1988, hereafter PSK) observed M81 at Hα with the Courtes f/1 focal reducer at the 6 m telescope of the (then) Soviet Special Astrophysical Observa-

tory, compiling a catalog of 492 H II regions, and giving positions, sizes, and Hα fluxes. We have identified 46 of the brightest PSK H II regions with UV sources visible on both the near-UV and far-UV images. UV magnitudes for the 46 H II regions were measured using apertures of diameter 14 pixels (approximately 16″), applying aperture corrections determined from stellar profiles. V band fluxes were measured from our CCD image. H II region fluxes were corrected for local background by subtracting the modal flux with an annulus of width 8″.

The brightest H II region in both UV bands is number 311 in the PSK catalog, which is identified with Kaufman H II region number 181 and is also the brightest in Hα of the PSK H II regions. With observed far-UV flux 5.60×10^{-15} ergs cm^{-2} Å^{-1} s^{-1}, PSK 311 is about 100 times as luminous in the far-UV as the Orion Nebula, including the exciting stars. Here, we have assumed distances of 450 pc and 3.3 Mpc for Orion Nebula and M81, and have taken the UV flux of the Orion Nebula from Bohlin et al. (1982). The far-UV flux of PSK 311 is 0.66 that of the giant local group association NGC 206 in M31 (Hill et al. 1992), while the $m_{152} - m_{249}$ color is -1.00, compared with -0.77 for NGC 206.

The contributions to the measured UV and optical fluxes of the H II regions from atomic emission processes, including two-photon continuum recombination radiation, were estimated to be less than about 15% using the results of Brown & Mathews (1970). We have not made corrections for the atomic emission, since the average contribution of atomic emission is small and we lack the accurate extinction and Hα measures needed to do so.

Figure 5 plots $m_{152} - V$ versus $m_{249} - V$ for the 46 H II regions, rereddened using the individual A_v values of Kaufman et al. (1987) where possible or the average extinction of 1.1 mag for H II regions not observed by Kaufman et al. (1987), using the Galactic reddening curve (Savage & Mathis 1979). A model spectrum computed for an unreddened cluster of age 3 million yr, using the stellar evolution models of Maeder & Meynet (1987) together with the model atmospheres of Kurucz (1979), and assuming the initial mass function to be a power law with exponent -1.5 and upper mass limit 120 $M_\odot$, predicts $m_{152} - V \sim -4.3$, and $m_{249} - V \sim -3.0$. The blue end of the observed linear distribution of colors in Figure 5 is consistent with these predicted values. The colors predicted by the models are not sensitive to the power-law exponent. For example, $m_{152} - V$ only varies from -4.3 to -4.1 as the exponent varies from -1.0 to -2.0.

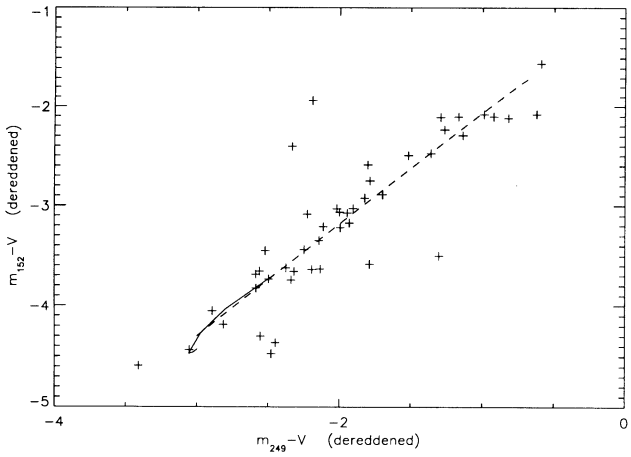

FIG. 5.—$m_{152} - V$ vs. $m_{249} - V$ colors for 46 PSK H II regions, dereddened using the A_v values of Kaufman *et al.* (1987). The solid line shows the expected positions of unreddened clusters with ages up to 5 Myr. The dashed line gives the expected positions of H II regions whose $E(B - V)$ values have been underestimated by 0.0 (*lower left*) to 0.5 mag (*upper right*).

The fact that most of the H II regions are redder than the colors expected from the model suggests that the A_v values have been underestimated by varying amounts. The dashed line in Figure 5 indicates the relationship expected between the colors if $E(B - V)$ has been underestimated by 0.0–0.5 mag. New A_v values were determined for the H II regions from the observed $m_{249} - V$, the expected color from the model, and the Galactic reddening curve (Savage & Mathis 1979).

It is also possible, in principle, for the redder observed UV colors to be caused by larger ages than the 3 Myr assumed by the model. The solid line shows the model positions for ages up to 5 Myr. The distribution is roughly parallel to the dashed reddening line. Although an increased age might be important in some cases, it is likely to be a minor effect in general, because the Lyman continuum flux computed by the same cluster model software decreases strongly for ages greater than 3 Myr. For age 5 Myr the ionizing flux is only ~0.25 of the flux at age 3 Myr.

An equivalent possibility is that redder H II region colors may result from a mass function with a lower mass limit than the 120 $M_\odot$ assumed heretofore. If the upper mass limit is decreased to 15 $M_\odot$, the colors $m_{152} - V$ and $m_{249} - V$ become -3.52 and -2.30, respectively. Only about a dozen of the H II regions could have their redder colors explained in this way, according to Figure 5.

The mean of the newly determined A_v values is 1.5 mag, consistent within the errors estimated by Kaufman et al. (1987) with their average A_v of 1.1. The extinction of the exciting stars may also be somewhat different from the extinction of the Hα emission from the recombining gas.

The mean $m_{152} - V$ after dereddening using the new A_v values is -4.3, consistent with the model spectrum. Therefore, we conclude that the Galactic reddening curve of Savage & Mathis (1979) describes the far-UV extinction of M81, as previously found for M83 (Bohlin et al. 1990).

4. SUMMARY

Ultraviolet images of M81 obtained by the UIT, together with ground-based optical data, allow determination of radial surface brightness profiles in bands centered at 2490 and 1520 Å, as well as the optical V band. The exponential disk, prominent in all three bands, dominates increasingly as the wavelength of observation decreases. Ultraviolet disk emission is suppressed interior to the ILR. Fluxes for 46 bright H II regions are determined in the three bands. Colors are consistent with models for young clusters reddened according to the Galactic reddening curve, with A_v greater by ~0.4 mag, on average than estimated previously from radio to Hα.

We gratefully acknowledge the innumerable contributions made by the hundreds of people involved in the *Astro-1* mission. R. W. O. gratefully acknowledges NASA support of portions of this research through grants NAG5-700 and NAGW-2596 to the University of Virginia.

REFERENCES

Bohlin, R. C., Cornett, R. H., Hill, J. K., & Stecher, T. P. 1990, ApJ, 363, 154
Bohlin, R. C., Hill, J. K., Stecher, T. P., & Witt, A. N. 1982, ApJ, 255, 87
Boroson, T. 1981, ApJS, 46, 177
Brown, R. L., & Mathews, W. G. 1970, ApJ, 160, 939
Code, A. D., & Welch, G. A. 1982, ApJ, 256, 1
Freeman, K. C. 1970, ApJ, 160, 811
Hill, J. K., et al. 1992, ApJ, in press
Kaufman, M., Bash, F. N., Hine, B., Rots, A. H., Elmegreen, D. M., & Hodge, P. W. 1989, ApJ, 345, 674
Kaufman, M., Bash, F., Kennicutt, R. C., & Hodge, P. W. 1987, ApJ, 319, 61
Kennicutt, R. C., & Hodge, P. W. 1980, ApJ, 241, 573
Kurucz, R. 1979, ApJS, 40, 1
Leisawitz, D., & Bash, F. N. 1982, ApJ, 259, 133
Maeder, A., & Meynet, G. 1987, A&A, 182, 243
O'Connell, R. W., et al. 1992, ApJ, in press
Petit, H., Sivan, J. P., & Karachentsev, I. D. 1988, A&AS, 74, 475 (PSK)
Savage, B. D., & Mathis, J. S. 1979, ARA&A, 17, 73
Stecher, T. P., et al. 1992, ApJ, in press
Visser, H. C. D. 1980a, A&A, 88, 149
———. 1980b, A&A, 88, 159